

domain (CD) of Tet1 (1367–2039 amino acids: aa), Tet2 (1044–1921aa) and Tet3 (697–1668aa) were generated by subcloning of the DNA fragments into BamHI and NotI sites for Tet1, EcoRI and XhoI sites for Tet2 or EcoRI and NotI sites for Tet3 of pcDNA4HisMax. Plasmids encoding Xpress-tagged mutants deficient in the catalytic domain ( $\Delta$ CD) of Tet1 (1–1366aa), Tet2 (1–1043aa) and Tet3 (1–696aa) were also generated. The Aid mutants, Aid $\Delta$ NES (1–187aa) and Aid $\Delta$ N26 (27–198aa), were subcloned into BamHI/XhoI-digested pcDNA4MycHis. We used the KOD plus mutagenesis kit (TOYOBO) to generate a point mutant for Aid (F193A) and mutants for the Tet family catalytic domain, which include Tet1CDm (D1652Y, D1654A), Tet2CDm (H1304Y, D1306A) and Tet3CDm (H950Y, D952A).

### Cell culture and cDNA transfection

Human embryonic kidney cells (HEK293FT) (Invitrogen) and human colon cancer cells (DLD-1) (American Type Culture Collection) were maintained in Dulbecco's modified Eagle's medium with 10% heat-inactivated fetal bovine serum. Both of them were transiently transfected with plasmid DNA by FuGENE6 (Promega) according to the manufacturer's instructions, followed by immunofluorescence or co-immunoprecipitation 48 h post-transfection, unless otherwise noted.

### Immunofluorescence

The cells were fixed and permeabilized with cold 100% methanol for 10 min on ice. For 5hmC staining, permeabilized cells were treated with 4 N HCl for 10 min, followed by 1.5 M Tris-HCl (pH 8.8) treatment for 10 min, before being blocked with 1% BSA. The cells were incubated with primary antibodies; anti-Xpress mouse monoclonal antibody (mAb) (Life Technologies), anti-Myc rabbit polyclonal antibody (MBL), anti-5hmC rabbit polyclonal antibody (Active Motif) or anti-Aicda rabbit polyclonal antibody (Abcam) overnight at 4°C, followed by Alexa Fluor-conjugated secondary antibodies (Life Technologies) for 1 h, and DAPI staining for 5 min at room temperature. After washing with PBS containing with 0.05% Tween 20, the samples were mounted by using the Prolong Gold Antifade Reagent (Life Technologies), followed by curing on a flat surface in the dark overnight at 4°C. For four color staining, a Zenon Alexa Fluor labeling kit (Life Technologies) was used. The images were captured by a confocal laser microscope (OLYMPUS, FV1000). To score the subcellular localization in DLD-1 cells, we counted all of the fluorescence positive cells on 4-well chamber dishes (BD). When using HEK293FT cells, we counted cells in randomly acquired fields on the 4-well chamber dishes. In the case of co-transfection, co-expressed cells were counted and scored according to the Tet localization. Scoring of the subcellular localization was performed as indicated in Fig. S1.

### Immunoprecipitation and immunoblotting

Transfected HEK293FT cells were lysed in EBC buffer (50 mM Tris-HCl pH 8.0, 120 mM NaCl and 0.5% NP40 for detecting Xpress-tagged protein, or 1.0% NP40 for detecting Myc-tagged protein) with a protease inhibitor cocktail (SIGMA). The cell lysates were incubated for 3 h at 4°C with Dynabeads M280 sheep anti-mouse IgG (VERITAS) which had been pre-treated with an anti-Xpress mAb or an anti-Myc mAb (Enzo life science) for 1 h. After washing the immunoprecipitates four times with EBC buffer, the beads were boiled with Laemmli SDS-sample buffer. This supernatant was separated by SDS-PAGE and transferred to a PVDF membrane (Millipore). For immunoblotting of the Xpress-tagged protein, after the membrane were blocked with 2% nonfat dry milk in PBS containing 0.05% Tween20, they were incubated

with an anti-Xpress mAb followed by anti-mouse IgG antibody conjugated to HRP specific for naive IgG (Novagen). For Myc-tagged protein blotting, after being blocked, the membrane was incubated with anti-Myc antibody conjugated to HRP (MBL). Each antibody was diluted in Can Get Signal for immunoblotting (TOYOBO). Protein bands were visualized using the Pierce ECL plus Western Blotting Substrate (Thermo), and detected with a LAS4000 instrument (GE HealthCare).

### Statistic analysis

The statistical significance of differences between two groups was determined by the Mann-Whitney U test. A value of  $p < 0.05$  was considered to be statistically significant. The numbers of samples are referred to as "n" in each graph.

## Results

### Aid alters the subcellular localization of Tet1 from the nucleus to the cytoplasm

A previous study showed that Tet family proteins generate 5hmC, whereas Aid facilitates the conversion of 5hmC into cytosine [9]. In this study, we investigated the effect of simultaneous expression of Aid and Tet on their subcellular localization. We transfected C-terminally Myc-tagged Aid or N-terminally Xpress-tagged Tet1 into HEK293FT or DLD-1 cells, and examined the subcellular localization of ectopically expressed proteins. Aid was observed mainly in the cytoplasm, whereas Tet1 was predominantly localized in the nucleus when the single proteins were overexpressed. When cells were co-transfected with expression plasmids for Aid and Tet1, the Tet1 localization was altered from the nucleus to the cytoplasm in the co-transfected cells, whereas Aid remained in the cytoplasm (Fig. 1).

To determine the domain responsible for the altered localization of Tet1, we performed a subcellular localization analysis using a series of deletion constructs for Tet1, as previously reported [17]; full length (FL) (1–2039 amino acids: aa) which was used in the experiment shown in Fig. 1, the catalytic domain (CD) (1367–2039aa), and the N-terminal domain ( $\Delta$ CD) (1–1366aa), which lacks CD (Fig. 2A). The Tet1FL plasmid and these mutants were transfected individually with or without the plasmid for Aid. At 48 hrs after transfection, the subcellular localization of Tet1 and Aid was examined by confocal microscopy (Figs. 2B and S2). In the case of single transfection, all Tet1 mutants were predominantly localized in the nucleus, and Aid was mainly localized in the cytoplasm. However, when Tet1FL or Tet1CD was co-expressed with Aid, Tet1 was translocated to the cytoplasm (N: 0%, N+C: 9%, C: 91% for FL, and N: 18%, N+C: 35%, C: 47% for CD, respectively). In contrast, Tet1 $\Delta$ CD remained in the nucleus even when co-expressed with Aid (N: 75%, N+C: 19%, C: 6%), suggesting that the catalytic domain of Tet1 plays a role in the altered localization of the protein (Figs. 2B and C). Since a previous study indicated that the subcellular localization of Aid is affected by the position of the tag [18], we also carried out co-transfection experiments using untagged Aid protein. It was confirmed that untagged Aid, as well as C-terminal-tagged Aid, also affected the localization of Tet1CD (Fig. S3), supporting the notion that Aid expression alters the subcellular localization of Tet1.

Next, to examine whether this effect is specific to Aid, we carried out the same experiments by using Apobec1 and Apobec2, instead of Aid, both of which show the similar enzymatic activity to Aid [19,20]. In particular, Apobec1 has been shown to shuttle between the nucleus and the cytoplasm [21]. We observed that overexpressed Apobec1 and Apobec2 were localized at both the

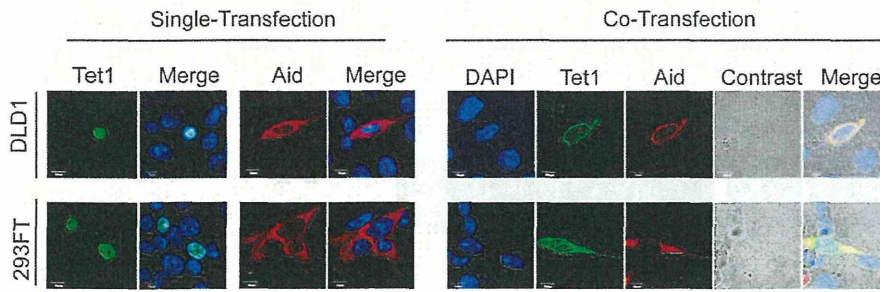


**Figure 1. Overexpressed Aid alters the subcellular localization of Tet1.** Images of cells transiently expressing N-terminally Xpress-tagged Tet1 or C-terminally Myc-tagged Aid. Tet1 was predominantly localized in the nucleus, whereas Aid was mainly localized in the cytoplasm 48 h after transfection in both DLD-1 and HEK293FT cells. When cells were co-transfected with a plasmid expressing Aid, the Tet1 subcellular localization was altered to the cytoplasm, where Aid was mainly localized. The scale bar is 10  $\mu$ m. doi:10.1371/journal.pone.0045031.g001

nucleus and the cytoplasm in DLD-1 cells regardless of the presence or absence of Tet1CD (Figs. S4). In contrast to the translocation of Tet1CD in the presence of Aid, Tet1CD always remained in the nucleus even when co-expressed with Apobec1 or Apobec2 (Figs. S4B and D,  $p=0.11$ , with vs without Apobec1,  $p=0.38$ , with vs without Apobec2). These results suggest that the altered subcellular localization of Tet1CD is not attributable to the artificial effects due to Aid overexpression.

**Tet1 translocation is independent of its enzymatic activity**

We observed that the subcellular localization of Tet1 was altered in the presence of Aid, but that Tet1 $\Delta$ CD remained in the nucleus, implying that Tet1 enzymatic activity for the conversion of 5mC to 5hmC is associated with the translocation of Tet1. To test this, a Tet1CD mutant construct (CDm), which has mutations

in the catalytic domain (D1652Y and D1654A) and lacks enzymatic activity, was generated (Fig. 3A) [17]. When Tet1CDm was solely transfected into DLD-1 cells, it was localized in the nucleus. However, the enzyme activity, which was detected by immunostaining for 5hmC, was not observed at all in Tet1CDm-expressing cells while it was evident in Tet1CD- and Tet1 FL-expressing cells (Fig. 3B). We also confirmed that Tet1 $\Delta$ CD and Aid had no ability to produce 5hmC (Figs. 3B and S5A).

We next examined the subcellular localization of Tet1CDm when it was co-expressed with Aid in DLD-1 cells. Despite the lack of enzymatic activity in Tet1CDm, simultaneous expression of Aid and Tet1CDm caused the altered localization of Tet1CDm, and no significant difference in the localization of Tet1CD and Tet1CDm was observed when they were co-expressed with Aid ( $p=0.144$ , CD vs CDm) (Figs. 2C and 3C). We obtained the similar observation using HEK293FT cells (Fig. S2). These results

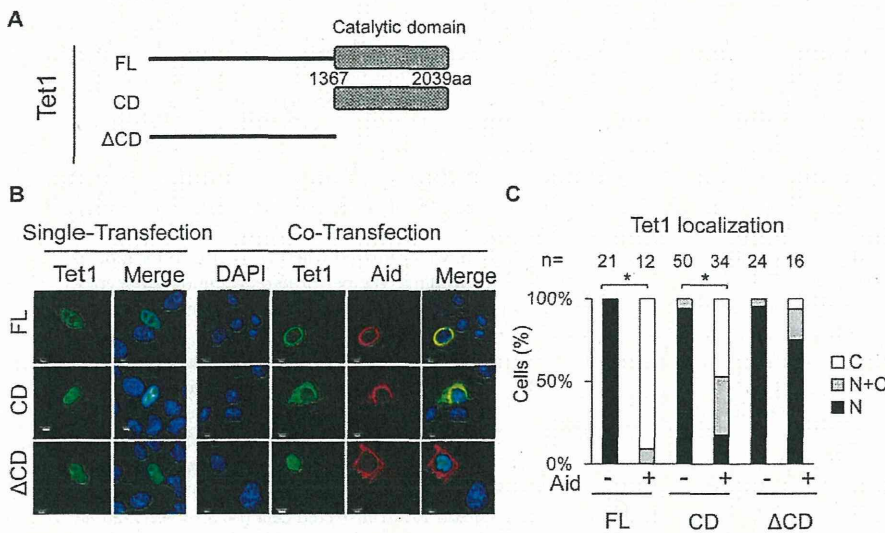


**Figure 2. Tet1 translocation requires its catalytic domain.** (A) A schematic representation of the Tet1 structure and its mutants used in this study. (aa = amino acid). (B) Confocal images of DLD-1 cells transiently expressing N-terminally Xpress-tagged Tet1 mutants with or without C-terminally Myc-tagged Aid. All Tet1 constructs (FL, CD and  $\Delta$ CD) were localized in the nucleus when solely expressed in DLD-1 cells. When co-expressed with Aid, Tet1FL and Tet1CD were translocated to the cytoplasm, whereas Tet1 $\Delta$ CD remained in the nucleus. (C) Each bar represents the proportion of cells with the different localizations of Tet1. The number (n) of cells indicated above each bar was scored according to their subcellular localization. N (black); nuclear localization, N+C (gray); both nuclear and cytoplasmic localization, C (white); cytoplasmic localization in multiple microscope fields. The scale bars in images are 10  $\mu$ m. \* $p<0.01$ . doi:10.1371/journal.pone.0045031.g002

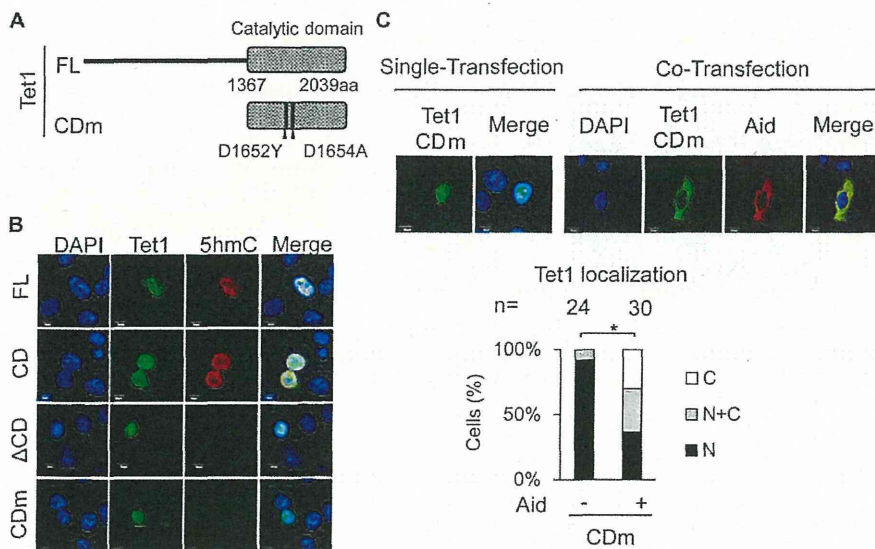


**Figure 3. Tet1 translocation in the presence of Aid is independent of the Tet1 enzymatic activity.** (A) A schematic representation of the Tet1CD mutant (CDm) used in this study. Tet1CDm were tagged with N-terminal Xpress. (B) Tet1FL and CD had enzyme activity and produced 5hmC, but Tet1ΔCD and CDm did not. (C) C-terminally Myc-tagged Aid expression altered the subcellular localization of Tet1CDm, which lacks the enzymatic activity. The upper panels are representative images of DLD-1 cells transiently expressing Tet1CDm with or without simultaneous expression of Aid. The lower graph shows the percentage score of the examined transfected cells (indicated as a number). The scale bars are 10 μm. \* $p < 0.01$ . N (black); nuclear localization, N+C (gray); both nuclear and cytoplasmic localization, C (white); cytoplasmic localization in multiple microscope fields.

doi:10.1371/journal.pone.0045031.g003

indicate that, although the catalytic domain of Tet1 is important for the Aid-mediated translocation of Tet1, the translocation occurs independently of its enzymatic activity.

#### Co-expression of Aid has similar effects on the subcellular localization of other Tet family proteins

The Tet family proteins include Tet1, Tet2 and Tet3. We therefore examined whether the effects of Aid co-expression were also observed for other Tet family members. To perform these studies, FL, CD, ΔCD and CDm constructs for both Tet2 and Tet3 were generated (Fig. 4A) based on a previous report [17], and their subcellular localization in the presence or absence of Aid was examined. In both Tet2 and Tet3, the FL and CD proteins exhibited enzymatic activity, whereas the ΔCD and CDm mutants did not (Fig. S5B). Single expression of Tet2FL or its mutants led to the localization of the proteins primarily in the nucleus (Figs. 4B and C). However, in solely Tet3-expressing cells, Tet3ΔCD showed cytoplasmic localization, even in the single transfectants, although Tet3FL, Tet3CD and Tet3CDm were localized in both the nucleus and the cytoplasm (Figs. 4D and E), indicating that the catalytic domain of Tet3 is responsible for the nuclear localization of Tet3. Simultaneous expression of Aid and either of Tet FL, CD or CDm resulted in the altered subcellular localization of both Tet2 and Tet3 into the cytoplasm (Figs. 4B–E). These findings suggest that Aid alters the subcellular localization of all three Tet family proteins, and that this occurs independently of enzyme activity to produce 5hmC.

#### Translocation of Tet1 by Aid is associated with Aid shuttling

We next addressed how nuclear Tet1 is translocated into the cytoplasm by Aid. To understand the mechanism, we first examined the localization of both Tet1CD and Aid at different

time points (10 h, 24 h, 48 h) after simultaneous transfection into HEK293FT cells. At 10 h after transfection, the subcellular localization of Tet1CD was mainly in the nucleus (N: 90%, N+C: 10%, C: 0%) while Aid was primarily expressed in the cytoplasm, showing the same localization pattern in the single transfected cells. At 24 h after transfection, the proportion of cells with cytoplasmic Tet1CD increased (N: 41%, N+C: 52%, C: 7%), and at 48 h after transfection, most of the Tet1CD were co-localized with Aid in the cytoplasm (N: 3%, N+C: 30%, C: 67%) (Figs. 5A and B). In contrast, Aid could be detected in the cytoplasm throughout this experiment.

It is worth noting that Aid is a shuttling protein that is translocating between the nucleus and the cytoplasm [12,13]. Since a gradual increase in the number of cells with cytoplasmic Tet1CD was observed, we evaluated whether Tet1 translocation is associated with Aid shuttling. We performed immunofluorescence experiment by using full length Aid (Aid FL) and its mutants which are impaired in nuclear-cytoplasmic shuttling; Aid lacking NES (AidΔNES\_1-187aa), Aid having a single point mutation in the NES (Aid F193A) [22] [23] or Aid lacking the N terminus of Aid, which loses the important sequences for nuclear entry (AidΔN26\_27-198aa) [12] (Fig. 6A). As expected, AidΔNES transfected cells revealed an increased number of cells with nuclear localization of Aid (ΔNES; N: 27%, N+C: 33%, C: 40%) when compared with Aid FL-transfected cells (N: 3%, N+C: 28%, C: 69%) (Figs. 6B and C). In addition, Aid F193A showed an increased localization of Aid at the nucleus (N: 23%, N+C: 43%, C: 34%) than Aid FL did. (Figs. 6B and D). Next, we co-transfected these Aid mutants with Tet1CD in DLD-1 cells and examined the effect of the expressions of Aid mutants on the Tet1CD subcellular localization (Figs. 6E and F). Co-expression with AidΔNES resulted in a decrease in the number of Tet1CD-translocated cells (N: 55%, N+C: 20%, C: 25%) compared with

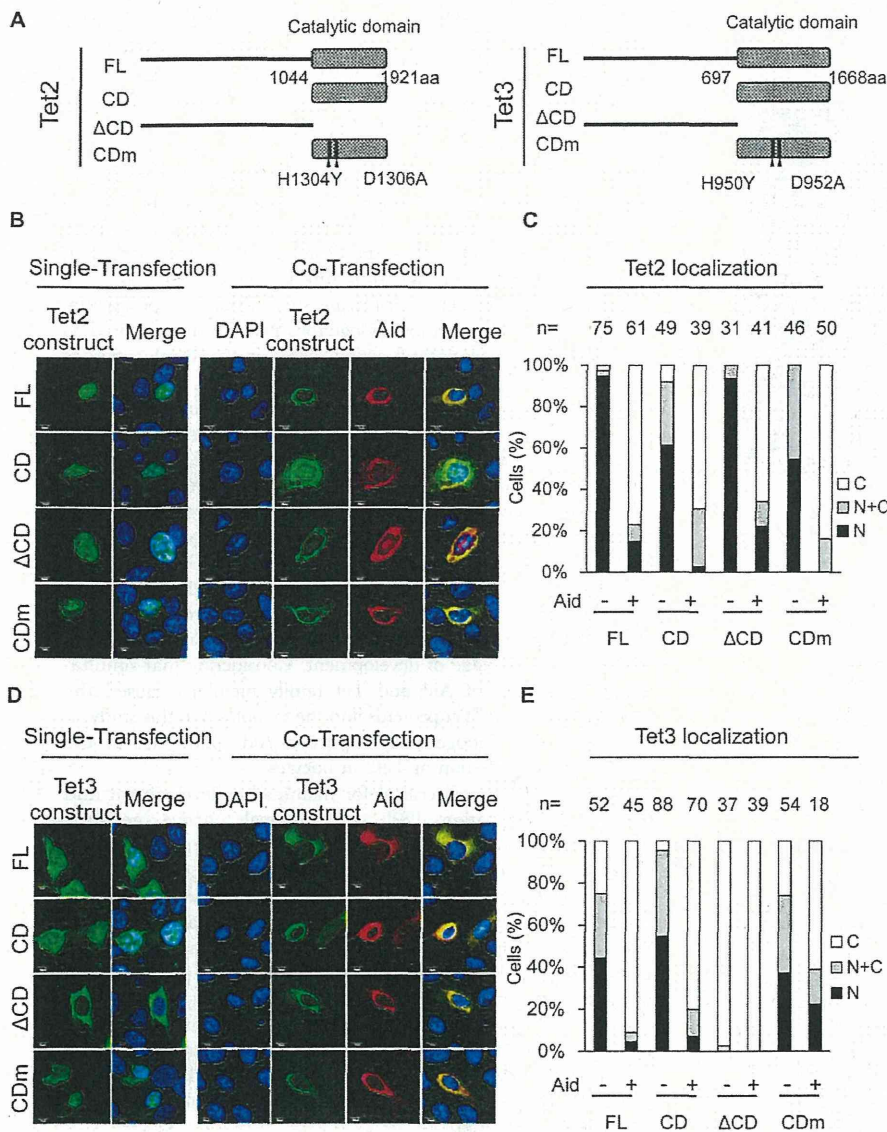


**Figure 4. The subcellular localization of Tet2 and Tet3 is altered by Aid expression.** (A) A schematic representation of the Tet2 and Tet3 structures and their mutants used in this study. (B) N-terminally Xpress-tagged Tet2 or its mutants with or without Aid tagged with C-terminal Myc were imaged by confocal microscopy in transiently transfected DLD-1 cells. (C) The number (n) of cells indicated above each bar was scored according to Tet2 subcellular localization. All Tet2 mutants were translocated to the cytoplasm in the presence of Aid ( $p < 0.01$ , vs in the absence of Aid). (D, E) Simultaneous expression of N-terminally Xpress-tagged Tet3 and Aid-Myc. Tet3FL, CD and CDm were translocated to the cytoplasm when co-expressed with Aid ( $p < 0.01$ , single-expression vs co-expression). Tet3 $\Delta$ CD was localized in the cytoplasm regardless of the Aid expression. The scale bars are 10  $\mu$ m. N (black); nuclear localization, N+C (gray); both nuclear and cytoplasmic localization, C (white); cytoplasmic localization in multiple microscope fields. doi:10.1371/journal.pone.0045031.g004

that induced by with Aid FL (N: 18%, N+C: 35%, C: 47%) (Figs. 2C and 6E). Similarly, when co-expressed with a single point mutant AidF193A, the proportion of Tet1CD-translocated cells were decreased (N: 57%, N+C: 17%, C: 26%) in comparison to those when co-transfected with Aid FL (Figs. 2C and 6F). In addition, we performed the similar experiment using Aid $\Delta$ N26, which has defect in nuclear entry. Aid $\Delta$ N26 was predominantly localized at the cytoplasm in the case of single expression (N: 0%, N+C: 5%, C: 95%) (Fig. 6G). When co-expressed with Aid $\Delta$ N26, Tet1CD remained in the nucleus (N: 72%, N+C: 24%, C: 4%)

(Figs. 2C and 6H). Taken together, these findings imply that Aid shuttling, which is mediated by the N-terminus and C-terminus domains of Aid, is associated with the Aid-mediated translocation of Tet1, and suggest that Tet1 translocation is dependent on the subcellular localization of Aid.

#### Interaction between Aid and Tet1

In this study, we found that nuclear Tet1 is translocated to the cytoplasm by Aid, and that the translocated Tet1 is co-localized with Aid. We next examined whether Aid interacts with Tet1

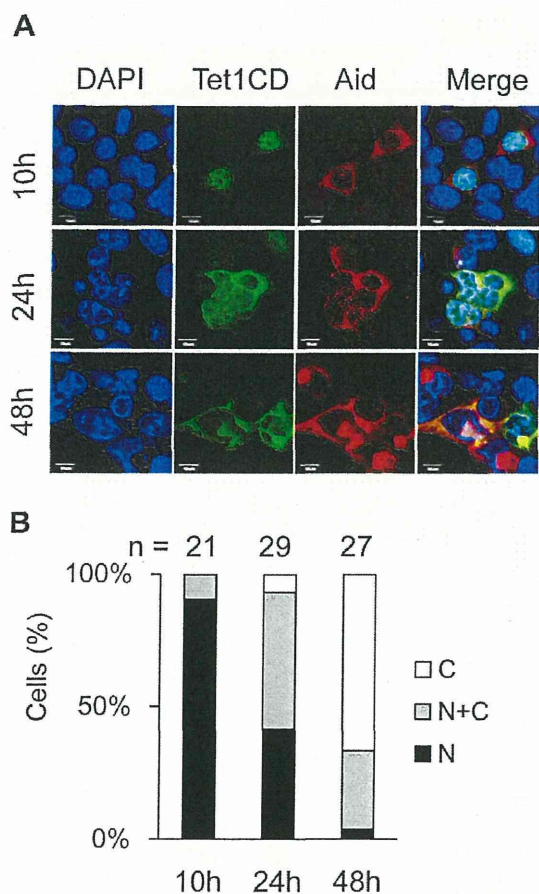


**Figure 5. Nuclear Tet1 is gradually translocated into the cytoplasm by the simultaneous expression of Aid.** (A) Confocal images of HEK293FT cells transiently co-expressing Tet1CD tagged with N-terminal Xpress and Aid tagged with C-terminal Myc at different time points (10 h, 24 h and 48 h) after co-transfection. The scale bars in images are 10  $\mu$ m. (B) The number (n) of cells indicated above each bar was scored according to the Tet1CD subcellular localization. The number of cells with cytoplasmic Tet1CD gradually increased after co-transfection. N (black); nuclear localization, N+C (gray); both nuclear and cytoplasmic localization, C (white); cytoplasmic localization in multiple microscope fields.  
doi:10.1371/journal.pone.0045031.g005

during this Aid-mediated translocation of Tet1. We carried out co-immunoprecipitation (co-IP) – immunoblotting (IB) using HEK293FT cells transfected with either or both the Xpress-Tet1CD and Aid FL-Myc vectors. Empty vectors were used as a negative control. Aid FL-Myc was co-precipitated with an anti-Xpress mAbs for Xpress-Tet1CD, and this association was confirmed by reciprocal IP with anti-Myc mAbs (Fig. 7A). Moreover, we observed a decreased interaction of Aid $\Delta$ NES with Tet1CD, although both Aid $\Delta$ NES and Tet1CD were localized in the nucleus (Fig. 7B). This result indicates that the NES domain of Aid is associated with the interaction between Aid and Tet1.

## Discussion

Aid shuttles between the nucleus and the cytoplasm, interacting with several molecules, such as RNA polymerase II [24], CTNBL-1 [25] and GANP [26], in order to target the IgV

region and/or the S region DNA. Previous studies proposed that the shuttling of Aid plays a role in preventing excessive DNA mutation in the nucleus [18,27]. In the present study, we showed that the simultaneous expression of Aid and Tet family enzymes causes the altered subcellular localization of the Tet family proteins. Furthermore, the translocation of Tet was affected by Aid shuttling between the nucleus and the cytoplasm. These results suggest that Aid shuttling might have another function; altering the subcellular localization of Tet family members. However, it should be also noted that the level of Aid induced in this experiment seems to be substantially higher than that of physiological condition. Considering such artificial experimental system, further analyses for endogenous proteins are required to conclude the physiological function of Aid in the translocation of Tet family enzymes.

Although the physiological relevance of our findings remains to be established, it is important to note that the expression of both Tet family proteins and Aid is restricted to specific cell types. It was reported that Aid is highly expressed in oocytes [28], while Tet3 is expressed at high levels in oocytes and zygotes [6], thus indicating that both Tet3 and Aid are abundantly expressed in oocytes. Of note, Tet3 is localized in the cytoplasm in oocytes, but it translocates into the male pronucleus of zygotes shortly after fertilization [16]. Therefore, it seems that there is dynamic regulation of the subcellular localization of Tet family members during the early stage of development. Considering that simultaneous expression of Aid and Tet family members caused the translocation of Tet proteins into the cytoplasm in this study, it is possible that endogenously expressed Aid contributes to the cytoplasmic localization of Tet3 in oocytes.

DNA methylation is critical for mammalian development and cellular differentiation [29]. In mammals, active genomic demethylation contributes to the genome-wide erasure of the DNA methylation observed in preimplantation embryos and primordial germ cells (PGCs) [30,31]. However, the mechanisms underlying active DNA demethylation in mammals have been highly controversial, although multiple mechanisms have been proposed [32–34]. Recently, an additional model was reported, wherein Aid facilitates the conversion of 5hmC into cytosine [9,35], and forms several complexes with thymine DNA glycosylase and GADD45a, which are involved in active DNA demethylation [36]. Our findings may also support the notion that Aid plays a role in DNA demethylation while interacting with several related factors.

To determine whether the altered subcellular localization of Tet contributes to the altered production of 5hmC, we performed immunodetection for 5hmC in dually-transfected cells (expressing both Tet1 and Aid), where Tet1 was translocated into the cytoplasm. Although Tet1 CD had already been translocated into the cytoplasm, 5hmC was still detectable in the nucleus (Fig. S6). Therefore, we could not conclude whether the translocation of Tet can affect the production of 5hmC in cells expressing both proteins. One of the possible explanations for our observation is that 5hmC is, to some extent, stable after its production, which made it difficult to detect an alteration in the 5hmC levels under our experimental conditions.

In summary, our present findings indicate that Aid regulates the subcellular localization of Tet family proteins, and that this is associated with Aid shuttling. The subcellular localization of proteins is crucial for their functional activity and is associated with their functional diversity [37,38]. Since both Aid and the Tet family proteins are involved in the modification of 5hmC, the coordinated action of these proteins might control epigenetic modifications by affecting the subcellular localization of Tet family



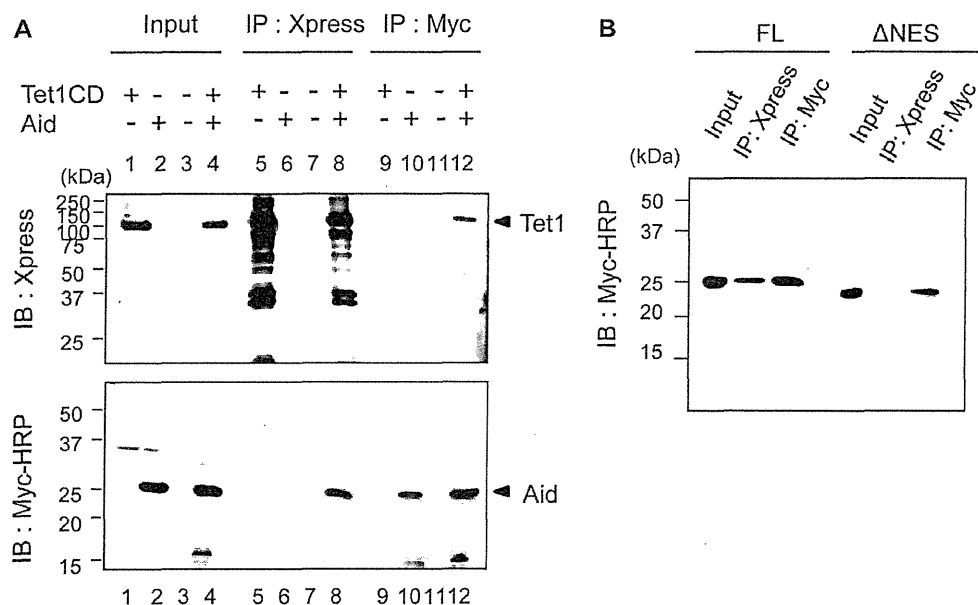


**Figure 7. Aid interacts with Tet1CD.** (A) Tet1CD was co-immunoprecipitated with Aid FL. Lysates from HEK293FT cells transfected with N-terminally Xpress-tagged Tet1CD, C-terminally Myc-tagged AidFL or both of them were immunoprecipitated (IP) by anti-Xpress mAbs or anti-Myc mAbs. Immunoblotting (IB) was performed by using an anti-Xpress Abs or anti-Myc-HRP antibody. Lane nos. 1, 5 and 9 were single transfections of Tet1CD. Lane nos. 2, 6 and 10 were single-transfections of Aid. Lane nos. 3, 7 and 11 were for mock transfection. Lane nos. 4, 8 and 12 shows the results for the co-transfection of Tet1CD and Aid. (B) The Co-IP experiment was performed by using lysates from HEK293FT cells co-transfected with N-terminally Xpress tagged-Tet1CD and C-terminally Myc-tagged Aid FL, or with N-terminally Xpress-tagged Tet1CD and C-terminally Myc-tagged AidΔNES. Despite the similar localization of AidΔNES and Tet1CD in the nucleus, AidΔNES revealed a decreased association with Tet1CD compared to Aid FL.

doi:10.1371/journal.pone.0045031.g007

proteins as we described in this study. Further studies are warranted to uncover the functional and physiological significance of the Aid-mediated translocation of Tet, which may eventually extend our understanding of the regulation of 5hmC production and active DNA demethylation.

## Supporting Information

**Figure S1 Representative images for each subcellular localization.** Representative images of each subcellular localization are shown. Dominant immunofluorescent signals in the nucleus and cytoplasm were regarded as nuclear localization (N) and cytoplasmic localization (C), respectively. Similar signal intensity in both the nucleus and the cytoplasm was regarded as C+N. Scale bars are 10 μm. (TIF)

**Figure S2 Aid alters the subcellular localization of Tet1 in HEK293FT cells.** HEK293FT cells expressing Aid also revealed translocation of Tet1CD and CDm. Consistent with the results in DLD-1 cells, Tet1ΔCD was retained in the nucleus even in the presence of Aid. The scale bars are 10 μm. (TIF)

**Figure S3 Untagged Aid expression results in the subcellular translocation of Tet1.** Untagged Aid was detected by an anti-Aid polyclonal antibody. Untagged Aid was mainly localized in the cytoplasm, which was the same as Myc-tagged Aid. Simultaneous expression of untagged Aid and Tet1CD caused the altered localization of Tet1CD in the cytoplasm. The scale bars are 10 μm. (TIF)

**Figure S4 Apobec family has not an effect on the subcellular localization of Tet1.** (A) The upper figures were confocal images of DLD-1 cells transiently expressing C-terminally Myc-tagged Apobec1. The lower graph represents the proportion of cells with different subcellular localization of Apobec1. (B) The upper figures were images of DLD-1 cells transiently co-expressing C-terminally Myc-tagged Apobec1 and N-terminally Xpress-tagged Tet1CD. The lower graph represents the percentage of the different subcellular localization of Tet1CD on the co-expressing cells. (C) The upper was images of DLD-1 cells transiently expressing C-terminally Myc-tagged Apobec2. The lower represents the proportion of cells with different subcellular localization of Apobec2. (D) The upper were images of DLD-1 cells transiently co-expressing C-terminally Myc-tagged Apobec2 and N-terminally Xpress-tagged Tet1CD. The lower showed the proportion of cells with different subcellular localization of Tet1CD on the co-expressing cells. The scale bars are 10 μm. N (black); nuclear localization, N+C (gray); both nuclear and cytoplasmic localization, C (white); cytoplasmic localization in multiple microscope fields. (TIF)

**Figure S5 Detection of 5hmC by immunostaining using in DLD-1 cells.** (A) Aid alone could not produce 5hmC. (B) The FL and CD had enzymatic activity, whereas the ΔCD and CDm proteins did not in both Tet2 and Tet3. Aid was tagged with C-terminal Myc and Tets were with N-terminal Xpress. The scale bars are 10 μm. (TIF)

**Figure S6 5hmC remains in the nucleus even after Tet1CD transfer to the cytoplasm in HEK293FT cells.**

The 5hmC could be still detected in the nucleus, even though Tet1CD was translocated from the nucleus to the cytoplasm in the presence of Aid. Aid was tagged with C-terminal Myc and Tets were with N-terminal Xpress. The scale bars are 20  $\mu$ m.

(TIF)

**Table S1 Primer sets for cloning Tet family and Aid used in this study.** F: forward primer, R: reverse primer (DOC)

**References**

1. Bird A (2002) DNA methylation patterns and epigenetic memory. *Genes Dev* 16: 6–21.
2. Goll MG, Bestor TH (2005) Eukaryotic cytosine methyltransferases. *Annu Rev Biochem* 74: 481–514.
3. Chen T, Li E (2004) Structure and function of eukaryotic DNA methyltransferases. *Curr Top Dev Biol* 60: 55–89.
4. Reik W, Dean W, Walter J (2001) Epigenetic reprogramming in mammalian development. *Science* 293: 1089–1093.
5. Inoue A, Zhang Y (2011) Replication-dependent loss of 5-hydroxymethylcytosine in mouse preimplantation embryos. *Science* 334: 194.
6. Iqbal K, Jin SG, Pfeifer GP, Szabó PE (2011) Reprogramming of the paternal genome upon fertilization involves genome-wide oxidation of 5-methylcytosine. *Proc Natl Acad Sci U S A* 108: 3642–3647.
7. Wossidlo M, Nakamura T, Lepikhov K, Marques CJ, Zakhartchenko V, et al. (2011) 5-Hydroxymethylcytosine in the mammalian zygote is linked with epigenetic reprogramming. *Nat Commun* 2: 241.
8. Tahiliani M, Koh KP, Shen Y, Pastor WA, Bandukwala H, et al. (2009) Conversion of 5-methylcytosine to 5-hydroxymethylcytosine in mammalian DNA by MLL partner TET1. *Science* 324: 930–935.
9. Guo JU, Su Y, Zhong C, Ming GL, Song H (2011) Hydroxylation of 5-methylcytosine by TET1 promotes active DNA demethylation in the adult brain. *Cell* 145: 423–434.
10. Di Noia JM, Neuberger MS (2007) Molecular mechanisms of antibody somatic hypermutation. *Annu Rev Biochem* 76: 1–22.
11. Muramatsu M, Kinoshita K, Fagarasan S, Yamada S, Shinkai Y, et al. (2000) Class switch recombination and hypermutation require activation-induced cytidine deaminase (AID), a potential RNA editing enzyme. *Cell* 102: 553–563.
12. Ito S, Nagaoka H, Shinkura R, Begum N, Muramatsu M, et al. (2004) Activation-induced cytidine deaminase shuttles between nucleus and cytoplasm like apolipoprotein B mRNA editing catalytic polypeptide I. *Proc Natl Acad Sci U S A* 101: 1975–1980.
13. Patenaude AM, Di Noia JM (2010) The mechanisms regulating the subcellular localization of AID. *Nucleus* 1: 325–331.
14. Rada C, Jarvis JM, Milstein C (2002) AID-GFP chimeric protein increases hypermutation of Ig genes with no evidence of nuclear localization. *Proc Natl Acad Sci U S A* 99: 7003–7008.
15. Yang G, Obiakor H, Sinha RK, Newman BA, Hood BL, et al. (2005) Activation-induced deaminase cloning, localization, and protein extraction from young VH-mutant rabbit appendix. *Proc Natl Acad Sci U S A* 102: 17083–17088.
16. Gu TP, Guo F, Yang H, Wu HP, Xu GF, et al. (2011) The role of Tet3 DNA dioxygenase in epigenetic reprogramming by oocytes. *Nature* 477: 606–610.
17. Ito S, D'Alessio AC, Taranova OV, Hong K, Sowers LC, et al. (2010) Role of Tet proteins in 5mC to 5hmC conversion, ES-cell self-renewal and inner cell mass specification. *Nature* 466: 1129–1133.
18. Patenaude AM, Orthwein A, Hu Y, Campo VA, Kavli B, et al. (2009) Active nuclear import and cytoplasmic retention of activation-induced deaminase. *Nat Struct Mol Biol* 16: 517–527.
19. Conticello SG (2008) The AID/APOBEC family of nucleic acid mutators. *Genome Biol* 9: 229.
20. Navaratnam N, Sarwar R (2006) An overview of cytidine deaminases. *Int J Hematol* 83: 195–200.

**Acknowledgments**

We are grateful to Drs. Takuya Yamamoto and Masamitsu Sone (CiRA) for helpful comments on this study, and to Drs. Minoru Yoshida (RIKEN) and Kazutoshi Takahashi (CiRA) for gifting materials. We also appreciate the members of the Yamada lab and Saito lab for their support.

**Author Contributions**

Conceived and designed the experiments: YA AW KS YY. Performed the experiments: YA. Analyzed the data: YA AW YY. Wrote the paper: YA AW YY.

21. Chester A, Somasekaram A, Tzimina M, Jarmuz A, Gisbourne J, et al. (2003) The apolipoprotein B mRNA editing complex performs a multifunctional cycle and suppresses nonsense-mediated decay. *EMBO J* 22: 3971–3982.
22. McBride KM, Barreto V, Ramiro AR, Stavropoulos P, Nussenzweig MC (2004) Somatic hypermutation is limited by CRM1-dependent nuclear export of activation-induced deaminase. *J Exp Med* 199: 1235–1244.
23. Geisberger R, Rada C, Neuberger MS (2009) The stability of AID and its function in class-switching are critically sensitive to the identity of its nuclear-export sequence. *Proc Natl Acad Sci U S A* 106: 6736–6741.
24. Nambu Y, Sugai M, Gonda H, Lee CG, Kataki T, et al. (2003) Transcription-coupled events associating with immunoglobulin switch region chromatin. *Science* 302: 2137–2140.
25. Conticello SG, Ganesh K, Xue K, Lu M, Rada C, et al. (2008) Interaction between antibody-diversification enzyme AID and spliceosome-associated factor CTNNB1. *Mol Cell* 31: 474–484.
26. Maeda K, Singh SK, Eda K, Kitabatake M, Pham P, et al. (2010) GANP-mediated recruitment of activation-induced cytidine deaminase to cell nuclei and to immunoglobulin variable region DNA. *J Biol Chem* 285: 23945–23953.
27. Stavtzev J (2011) Complex regulation and function of activation-induced cytidine deaminase. *Trends Immunol* 32: 194–201.
28. Morgan HD, Dean W, Coker HA, Reik W, Petersen-Mahrt SK (2004) Activation-induced cytidine deaminase deaminates 5-methylcytosine in DNA and is expressed in pluripotent tissues: implications for epigenetic reprogramming. *J Biol Chem* 279: 52353–52360.
29. Sasaki H, Matsui Y (2008) Epigenetic events in mammalian germ-cell development: reprogramming and beyond. *Nat Rev Genet* 9: 129–140.
30. Guibert S, Forné T, Weber M (2012) Global profiling of DNA methylation erasure in mouse primordial germ cells. *Genome Res*.
31. Zaitseva I, Zaitsev S, Alenina N, Bader M, Krivokharchenko A (2007) Dynamics of DNA-demethylation in early mouse and rat embryos developed in vivo and in vitro. *Mol Reprod Dev* 74: 1255–1261.
32. Rai K, Huggins IJ, James SR, Karpf AR, Jones DA, et al. (2008) DNA demethylation in zebrafish involves the coupling of a deaminase, a glycosylase, and gadd45. *Cell* 135: 1201–1212.
33. Bhutani N, Brady JJ, Damian M, Sacco A, Corbel SY, et al. (2010) Reprogramming towards pluripotency requires AID-dependent DNA demethylation. *Nature* 463: 1042–1047.
34. Popp C, Dean W, Feng S, Cokus SJ, Andrews S, et al. (2010) Genome-wide erasure of DNA methylation in mouse primordial germ cells is affected by AID deficiency. *Nature* 463: 1101–1105.
35. Bhutani N, Burns DM, Blau HM (2011) DNA demethylation dynamics. *Cell* 146: 866–872.
36. Cortellino S, Xu J, Sannai M, Moore R, Caretti E, et al. (2011) Thymine DNA glycosylase is essential for active DNA demethylation by linked deamination-base excision repair. *Cell* 146: 67–79.
37. Hung MC, Link W (2011) Protein localization in disease and therapy. *J Cell Sci* 124: 3381–3392.
38. Butler GS, Overall CM (2009) Proteomic identification of multitasking proteins in unexpected locations complicates drug targeting. *Nat Rev Drug Discov* 8: 935–948.



Development 139, 667-677 (2012) doi:10.1242/dev.072272  
 © 2012. Published by The Company of Biologists Ltd

# Genetic ablation of *Rest* leads to in vitro-specific derepression of neuronal genes during neurogenesis

Hitomi Aoki<sup>1</sup>, Akira Hara<sup>2</sup>, Takumi Era<sup>3</sup>, Takahiro Kunisada<sup>1</sup> and Yasuhiro Yamada<sup>4,5,\*</sup>

## SUMMARY

*Rest* (RE1-silencing transcription factor, also called *Nrsf*) is involved in the maintenance of the undifferentiated state of neuronal stem/progenitor cells in vitro by preventing precocious expression of neuronal genes. However, the function of *Rest* during neurogenesis in vivo remains to be elucidated because of the early embryonic lethal phenotype of conventional *Rest* knockout mice. In the present study, we have generated *Rest* conditional knockout mice, which allow the effect of genetic ablation of *Rest* during embryonic neurogenesis to be examined in vivo. We show that *Rest* plays a role in suppressing the expression of neuronal genes in cultured neuronal cells in vitro, as well as in non-neuronal cells outside of the central nervous system, but that it is dispensable for embryonic neurogenesis in vivo. Our findings highlight the significance of extrinsic signals for the proper intrinsic regulation of neuronal gene expression levels in the specification of cell fate during embryonic neurogenesis in vivo.

**KEY WORDS:** *Rest* (*Nrsf*), Mouse model, Neurogenesis

## INTRODUCTION

The establishment and maintenance of neuronal identity underlie the core of neuronal development. The transcriptional repressor RE1-silencing transcription factor [*Rest*; also known as neuron-restrictive silencer factor (*Nrsf*)], was initially discovered as a negative regulator of neuron-specific genes in non-neuronal cells (Chong et al., 1995; Schoenherr and Anderson, 1995). *Rest* is expressed throughout early development, where it represses the expression of neuronal genes and is involved in the transcriptional silencing of neuronal promoters in conjunction with *CoRest* (*Rcor1/2*) (Ballas et al., 2001), which recruits additional silencing machinery, including the methyl DNA-binding protein MeCP2, histone deacetylase (HDAC) and the histone H3K9 methyltransferase G9a (*Ehmt2*) (Andres et al., 1999; Lunyak et al., 2002; Roopra et al., 2004; Shi et al., 2003; You et al., 2001). *Rest* targets include a number of genes encoding ion channels, neurotrophins, synaptic vesicle proteins and neurotransmitter receptors (Bruce et al., 2004; Johnson et al., 2006; Otto et al., 2007). Indeed, a targeted mutation of *Rest* in mice caused derepression of neuron-specific tubulin in a subset of non-neuronal tissues, leading to embryonic lethality (Chen et al., 1998).

Mosaic inhibition of *Rest* in chicken embryos using a dominant-negative form of *Rest* also caused derepression of neuronal tubulin, as well as several other neuronal target genes, not only in non-neuronal tissues but also neuronal progenitors (Chen et al., 1998). These results suggest that *Rest* is required to repress the expression of neuronal genes in undifferentiated neuronal tissue. Expression

of *Rest* is highest in embryonic stem cells (ESCs) and is downregulated as ESCs differentiate into neuronal stem cells (NSCs), and it is completely silenced in mature adult neuronal cells (Ballas et al., 2005). Given the fact that *Rest* represses the expression of a large number of neuronal genes, it is reasonable to expect that it plays a central role in the inhibition of the precocious expression of neuronal genes in NSCs, and that its downregulation upon receipt of neuronal differentiation cues permits the robust expression of differentiation-related neuronal genes, resulting in terminal differentiation (Ballas et al., 2005).

In addition to the involvement of *Rest* in neurogenesis, recent studies have demonstrated that *Rest* modulates glial lineage elaboration (Abrajano et al., 2009; Kohyama et al., 2010), suggesting that it also mediates the coupling of neurogenesis and gliogenesis, which might contribute to the neuronal-glia interactions that are associated with synaptic and neuronal network plasticity and homeostasis in the brain. Despite the expectation of a fundamental role of *Rest* in brain development, the function of *Rest* in NSCs and neuronal progenitors in the brain in vivo remains to be elucidated. *Rest* null mice survive to embryonic day (E) 9 without obvious morphological defects, by which time all three germ layers and the neural tube have formed, clearly demonstrating that neuronal progenitors can develop in vivo in the absence of *Rest* (Chen et al., 1998). However, *Rest* null mice die by E11.5 accompanied by gross morphological changes starting ~E9.5. This early embryonic lethality has precluded further analysis of the role of *Rest* in the maintenance and differentiation of NSCs and neural progenitor cells (NPCs) in vivo.

In addition to the possible role of *Rest* in neuronal/glia development, recent studies have indicated that the breakdown of these processes accompanies and promotes neurodegenerative disorders. The disruption of the interaction of *Rest* with its target genes was reported in epileptic seizures (Bassuk et al., 2008), Huntington's disease (Zuccato et al., 2007) and Down's syndrome (Canzonetta et al., 2008; Lepagnol-Bestel et al., 2009). In these disorders, *Rest* dysfunction is suggested to be a cause of aberrant changes in neuronal gene expression. Considering that abnormal expression of *Rest* has been seen in a variety of neurological and neurodegenerative diseases, it is important to uncover the

<sup>1</sup>Department of Tissue and Organ Development and <sup>2</sup>Department of Tumor Pathology, Regeneration, and Advanced Medical Science, Gifu University Graduate School of Medicine, Gifu, 501-1194, Japan. <sup>3</sup>Division of Molecular Neurobiology, Institute of Molecular Embryology and Genetics, Kumamoto University, Kumamoto 860-0811, Japan. <sup>4</sup>PRESTO, Japan Science and Technology Agency, 4-1-8 Honcho Kawaguchi, Saitama, Japan. <sup>5</sup>Center for iPS Cell Research and Application (CiRA), Institute for Integrated Cell-Material Sciences (iCeMS), Kyoto University, Kyoto 606-8507, Japan.

\*Author for correspondence (y-yamada@cira.kyoto-u.ac.jp)

mechanisms that underlie how *Rest* suppresses the expression of neuronal genes to control neurogenesis and gliogenesis, and to provide a better understanding of the pathogenesis of such diseases.

In the present study, we have generated *Rest* conditional knockout mice that allow the effects of genetic ablation of *Rest* on brain development to be examined in vivo. We also examined the effect of *Rest* ablation in cells outside of the nervous system at different developmental stages.

## MATERIALS AND METHODS

### Animals

All animal experiments were approved by the Animal Research Committee of the Gifu University Graduate School of Medicine. *Rest*<sup>2lox/2lox</sup> mice were generated from the *Rest*<sup>2lox/+</sup> ESC line as described previously (Yamada et al., 2010). *Rosa26::rtTA*; *Coll1a1::tetO-Cre* mice (Yamada et al., 2010) and *Sox1-Cre*<sup>+</sup> mice (Takashima et al., 2007) were bred with *Rest*<sup>2lox/2lox</sup> mice to generate compound transgenic mice. In order to induce Cre recombinase, doxycycline (2 mg/ml) was administered in the drinking water of the mice, supplemented with 10 mg/ml sucrose (Hochedlinger et al., 2005). To induce Cre-*loxP* recombination in the embryos, pregnant female mice were treated with doxycycline in their drinking water for 5 days, and were sacrificed on the last day of the doxycycline administration. In order to label neuronal stem/progenitor cells in the adult brain, BrdU was administered as a daily intraperitoneal injection of 50 mg/kg body weight for 12 days starting at the age of 8 weeks. The brains were fixed 1 day after the last injection (Shi et al., 2004).

### Cell culture

For the neurosphere culture, brains were collected and dissociated into single-cell suspensions by gentle pipetting. The inner part of the trunk region was collected for genotyping. The primary neurospheres were formed from  $1 \times 10^5$  suspended brain cells/well in a 24-well plate. The cells were cultured in DMEM/F12 supplemented with  $1 \times N2$  (Invitrogen),  $1 \times B27$  (Invitrogen), 20 ng/ml epidermal growth factor (EGF) (R&D Systems) and 20 ng/ml basic fibroblast growth factor (bFGF, or FGF2) (R&D Systems). The primary neurospheres were passaged to generate secondary neurospheres, which were used to compare neurosphere formation ability. For the adherent cultures of neurospheres, the spheres were inoculated into 6-well plates previously coated with fibronectin/laminin (both from Invitrogen) and cultured in DMEM/F12 supplemented with  $1 \times B27$  and 10% fetal calf serum (FCS) (Nihirei Bioscience, Tokyo, Japan).

MEFs were derived from small pieces of the outer part of the trunk region prepared as described above. The cells were seeded in 100-mm dishes and cultured in DMEM supplemented with 10% FCS. In order to induce *Rest* recombination in vitro, cultured cells were treated with doxycycline at 2  $\mu$ g/ml. The cells were analyzed for GFP signals using a FACS Aria dual-laser flow cytometer (Becton-Dickinson).

### Histology and immunohistochemistry

The brains were enucleated and fixed by immersion overnight in 10% formalin in phosphate buffer (pH 7.2). Specimens were dehydrated with ethanol, soaked in xylene and embedded in paraffin. Horizontal serial sections were prepared at 3  $\mu$ m using a Leica RM2125RT microtome and stained with Hematoxylin and Eosin (HE).

For immunohistochemistry, we used a Mouse-to-Mouse HRP Ready-To-Use Kit (ScyTek Laboratories) according to the manufacturer's protocol to detect the mouse monoclonal primary antibodies on the sections. For detection of the goat or rabbit polyclonal primary antibodies, a Histofine Kit (Nihirei Bioscience, Tokyo, Japan) or VECTASTAIN ABC Kit (Vector Laboratories) was used according to the manufacturers' protocol. Finally, the sections were stained with 3,3'-diaminobenzidine (DAB). For immunocytochemistry studies, cells were fixed with 4% PFA, made permeable by immersion in 0.1% Triton X-100, washed in PBS and blocked in 0.5% BSA. Primary antibodies were then added and allowed to react for 60 minutes at room temperature. After washing in PBS, the cells were stained with secondary antibodies. Cells were examined using an Olympus IX-71 fluorescence microscope.

### Antibodies

The primary antibodies used in this study were: anti-mouse neuronal class III beta-tubulin (Tuj1; 1:5000; BabCO); anti-mouse glial fibrillary acidic protein (Gfap; 1:1000; Dako-Cytomation, Glostrup, Denmark); anti-human nestin (1:500; IBL, Gunma, Japan); anti-mouse nestin (1:1000; Chemicon); anti-mouse NeuN (1:1000; Chemicon); anti-BrdU (1:500; Dako-Cytomation); anti-doublecortin (Dcx; 1:500; Santa Cruz); anti-Prox1 (1:5000; Millipore); anti-radial glial cell marker 2 (clone RC2; 1:300; Millipore); anti-trimethyl histone H3 (Lys27) (1:200; Monoclonal Institute, Hokkaido, Japan).

### Gene expression analysis

Total RNA was prepared using the RNeasy Plus Mini Kit (Qiagen) according to the manufacturer's instructions. The first-strand cDNA was synthesized from 1  $\mu$ g total RNA using the SuperScript First-Strand Synthesis System (Takara, Shiga, Japan) with oligo(dT) primers. Real-time PCR was performed with SYBR Premix EX Taq (Takara) using Thermal Cycler Dice (Takara) for each gene of interest, and a  $\beta$ -actin endogenous control primer set was used for normalization. The primer sequences used in qRT-PCR analyses were obtained from PrimerBank (<http://pga.mgh.harvard.edu/primerbank/>).

The microarray analysis was performed according to the manufacturer's instructions (materials from Agilent unless otherwise stated). Briefly, cyanine-3 (Cy3)-labeled cRNA was prepared from 100 ng RNA using the One-Color Low RNA Input Liner Amplification Kit, followed by RNeasy column purification (Qiagen). Dye incorporation and cRNA yield were checked with a NanoDrop ND-1000 spectrophotometer. A total of 1.5  $\mu$ g of Cy3-labeled cRNA (specific activity  $>10.0$  pmol Cy3/ $\mu$ g cRNA) was fragmented at 60°C for 30 minutes in a reaction volume of 50  $\mu$ l containing  $1 \times$  fragmentation buffer and  $2 \times$  blocking agent following the manufacturer's instructions. On completion of the fragmentation reaction, 50  $\mu$ l  $2 \times$  HI-RPM Hybridization Buffer was added and hybridized to Whole Mouse Genome Oligo Microarrays (G4122F) for 17 hours at 65°C in a rotating hybridization oven. After hybridization, microarrays were washed for 1 minute at room temperature with GE Wash Buffer 1 and 1 minute at 37°C with GE Wash buffer 2, then dried immediately by brief centrifugation. Slides were scanned immediately after washing on a DNA microarray scanner (G2565B) using the one-color scan setting for 4 $\times$ 44k array slides [scan area 75 $\times$ 25 mm, scan resolution 5  $\mu$ m, dye channel set to green and green PMT set to 10-100% (XDR)]. The scanned images were analyzed with the Feature Extraction Software package v. 9.5.3.1 using default parameters (protocol GE1-v5\_95\_Feb07 and Grid: 014868\_D\_F\_20101102) to obtain background-subtracted and spatially detrended processed signal intensities. Data were analyzed using GeneSpring software.

## RESULTS

### Conditional ablation of the CoRest binding site in developing embryos results in embryonic lethality

In order to examine the effect of *Rest* deletion in vivo, we generated mice containing floxed *Rest* alleles and doxycycline-inducible *Cre* alleles (*Rest*<sup>2lox/2lox</sup>; *Rosa26::rtTA*; *Coll1a1::tetO-Cre*), in which exon 4, which encodes the CoRest binding site, can be removed upon treatment of mice with doxycycline (Fig. 1A) (Andres et al., 1999; Beard et al., 2006; Fink et al., 1999; Hatano et al., 2011; Yamada et al., 2010). *Rest* contains two repressor domains (Tapia-Ramirez et al., 1997): an N-terminal domain that associates with HDACs and Sin3; and a C-terminal domain that interacts with CoRest (Andres et al., 1999). Importantly, although our recombinant *Rest* knockout (KO) allele (*Rest*<sup>1lox</sup>) still contains exons 1-3, which encode the N-terminal domain of *Rest*, altered *Rest* transcript was not detected in our *Rest*<sup>1lox/1lox</sup> mouse ESCs, suggesting that the *Rest*<sup>1lox</sup> allele in this system is equivalent to the conventional KO allele (Yamada et al., 2010). We further demonstrated that *Stmn2* (*SCG10*), a CoRest-independent target of Rest-mediated repression (Jepsen et al., 2000; Lunyak et al., 2002),